A comparison of fully polarimetric X-band ISAR imagery of scaled model tactical targets

Thomas M. Goyette[*a], Jason C. Dickinson[a], Robert Giles[a], Jerry Waldman[a], William E. Nixon[b]

[a] Submillimeter-Wave Technology Laboratory, University of Massachusetts Lowell, 175 Cabot St, Lowell, MA 01854

[b] U.S. Army National Ground Intelligence Center, 2055 Boulders Road, Charlottesville, VA 22911

ABSTRACT

Construction of the new 350GHz compact range has been completed and it is able to collect fully polarimetric scaled X-band radar data with 6-inch full-scale range resolution. In order to investigate the reproduction of X-band data using scale models, fully polarimetric high-resolution radar signature data has been collected on several targets which include a high-fidelity in-house built 1/16th scale T72 Main Battle Tank (MBT) and a commercially available 1/35th scale model T72 modified to match its features. A correlation study of ISAR images has been performed between the X-band data sets collected on these models, a full-scale T72, a 1/35th scale model heavy equipment transporter, and several different 1/16th scaled targets of similar size. The ISAR images formed from the data were compared using several techniques which include a two-dimensional cross-correlation of the images against one another, and the comparison of the images pixel-by-pixel to measure the percentage differences. It will be shown that the T72 data sets compare well across the three different radar platforms. It has also been found that there are persistent sharp features in the two-dimensional cross-correlation maps that are located where the real target is matched even when other parameters have changed by a significant amount. These features continue to occur when the target has been imbedded in a complex two-target scene with the heavy equipment transporter.

Keywords: Radar, Imagery, Modeling, X-band

1. INTRODUCTION

Over the past twenty years the U. S. Army National Ground Intelligence Center (NGIC) and the University of Massachusetts Lowell (UML), under the Expert Radar Signatures Solutions (ERADS) program, have developed state-of-the-art scale model measurement systems to acquire high resolution radar signature data in support of a number of advanced radar applications. These applications include assisted target recognition (ATR), foliage penetration (FOPEN), and radar absorbing material (RAM) development. Compact ranges are now operating which model VHF/UHF, X-band, Ka-band, and W-band radar systems. ERADS most recent addition has been the installation of a fully polarimetric 350GHz compact range at UML to model X-band at 1/35th scale. The new 350GHz compact range provides complimentary capabilities to the 1/16th scale compact range operating at 160GHz. One benefit of a 1/35th scale compact range is the smaller physical size of the targets. This size permits the simulation of multi-target scenes.

Initially, simple objects were measured in the 350GHz compact range and the results were found to be in excellent agreement with predictions. Next a 1/35th scale-model T72 tank was made to copy as nearly as possible the configurations and features of the ERADS 1/16th scale model T72. Several test data collections were then performed on the 1/35th scale model T72 in several different operational configurations, and in a complex two-target scene wherein it was mounted to the back of a much larger vehicle. A comparison of the ISAR images was performed similar to the correlation studies done in previous works[1,2,3] where ISAR images are correlated against each other to determine the quality of the match. It will be shown that the T72 data sets correlate very well even across different radar platforms. Although placing the T72 into a complex scene changes the scattering significantly, results show that the target can still be identified by cross-correlation techniques. Additionally, certain features were observed in the two dimensional

[*] Correspondence: Email: Thomas_Goyette@uml.edu; Telephone: (978) 934-1380; Fax: (978) 452-3333.

Report Documentation Page

Form Approved
OMB No. 0704-0188

1. REPORT DATE	2. REPORT TYPE	3. DATES COVERED
MAY 2006		**00-00-2006 to 00-00-2006**

4. TITLE AND SUBTITLE	5a. CONTRACT NUMBER
A comparison of fully polarimetric X-band ISAR imagery of scaled model tactical targets	5b. GRANT NUMBER
	5c. PROGRAM ELEMENT NUMBER
6. AUTHOR(S)	5d. PROJECT NUMBER
	5e. TASK NUMBER
	5f. WORK UNIT NUMBER
7. PERFORMING ORGANIZATION NAME(S) AND ADDRESS(ES) **University of Massachusetts Lowell,Submillimeter-Wave Technology Laboratory,175 Cabot Street,Lowell,MA,01854**	8. PERFORMING ORGANIZATION REPORT NUMBER
9. SPONSORING/MONITORING AGENCY NAME(S) AND ADDRESS(ES)	10. SPONSOR/MONITOR'S ACRONYM(S)
	11. SPONSOR/MONITOR'S REPORT NUMBER(S)

12. DISTRIBUTION/AVAILABILITY STATEMENT
Approved for public release; distribution unlimited

13. SUPPLEMENTARY NOTES
The original document contains color images.

14. ABSTRACT

15. SUBJECT TERMS

16. SECURITY CLASSIFICATION OF:			17. LIMITATION OF ABSTRACT	18. NUMBER OF PAGES	19a. NAME OF RESPONSIBLE PERSON
a. REPORT	b. ABSTRACT	c. THIS PAGE			
unclassified	**unclassified**	**unclassified**		**10**	

cross-correlation maps of the images that occur where the target of interest was located. These features appear as sharp peaks that differ in comparison to the broad peaks that are observed when the wrong target is tested against the image. The sharp features persist even when the target is put into different operational environments. These observations will be discussed further in Section 4.

2. RADAR SIGNATURE DATA

The data used in this study fall into two separate categories and are listed in Table 1. The first category consists of data sets where the T72 MBT is the target of interest. These data files include measurements taken using a 1/35th-scale model, 1/16th-scale model, and full-scale T72. At 1/35th-scale a commercial model of the T72 was modified to match the features of the high-fidelity ERADS 1/16th-scale model. Additionally, the 1/35th-scale T72 was measured under several different conditions and configurations. Descriptions of the data sets are also included in Table 1. One of the data files has been taken as a complex two-target scene wherein the scale-model T72 tank was mounted on a larger heavy equipment transporter. This scene is shown in Figure 2.1. Another data set is a full-scale data collection produced at an outdoor radar turntable facility. There are also configuration differences between the T72 data sets that reflect differences in mounted hardware. The second category of data consists of targets that are not the T72. Data sets of two scale model targets that were of similar size to the T72 are also listed in Table 1. These sets include the 2S6 air defense unit and the T80 MBT.

File Number	Target	Scale Factor	Elevation	Illumination	Environment	Comment
1	T72	1/35	10˚	Far-Field	Desert	1st half of 720˚ spin
2	T72	1/35	10˚	Far-Field	Desert	2nd half of 720˚ spin
3	T72	1/35	10˚	Far-Field	Free-Space	T72 in Free Space
4	T72	1/16	10˚	Far-Field	Desert	T72 on ground plane
5	T72	Full	10˚	Near-Field	Free-Space	Turntable Measurement
6	HET/T72	1/35	10˚	Far-Field	Desert	T72 on back of HET
7	2S6	1/16	10˚	Far-Field	Desert	2S6 on ground plane
8	T80	1/16	10˚	Far-Field	Desert	T80 on ground plane

Table 1. List of data files used in the ISAR image cross-correlation analysis.

The measurements listed in Table 1 consist of fully polarimetric, high range resolution data. Heretofore we have limited the analysis of the ISAR images to the V-transmit V-receive (VV) polarization. However, preliminary correlation calculations show that the results for H-transmit H-receive (HH) polarization are very similar. Although the calculations have also been done for the HH channel, in the following sections discussions are limited to the VV polarization for brevity.

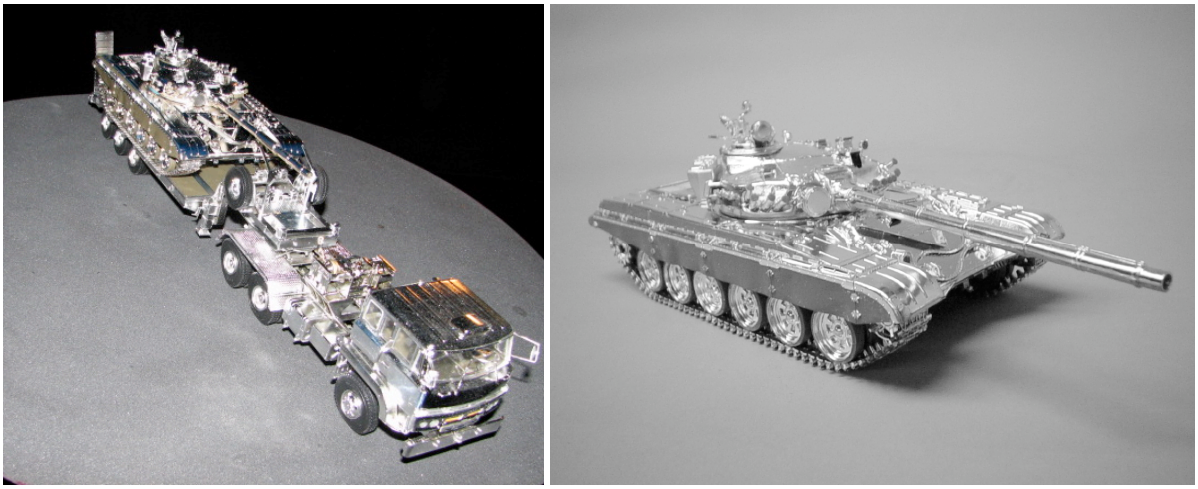

Figure 2.1. T72 model mounted on the Heavy Equipment Transporter (left) and alone (right)

3. ISAR IMAGE ANALYSIS

In order to aid in the description of the mathematical analysis a flow chart of the numerical technique is shown in Figure 3.1. The analysis is broken down into 7 major sections with different mathematics being performed in each section. The sections are numbered in the order in which they are performed. A detailed description of the various steps is listed below.

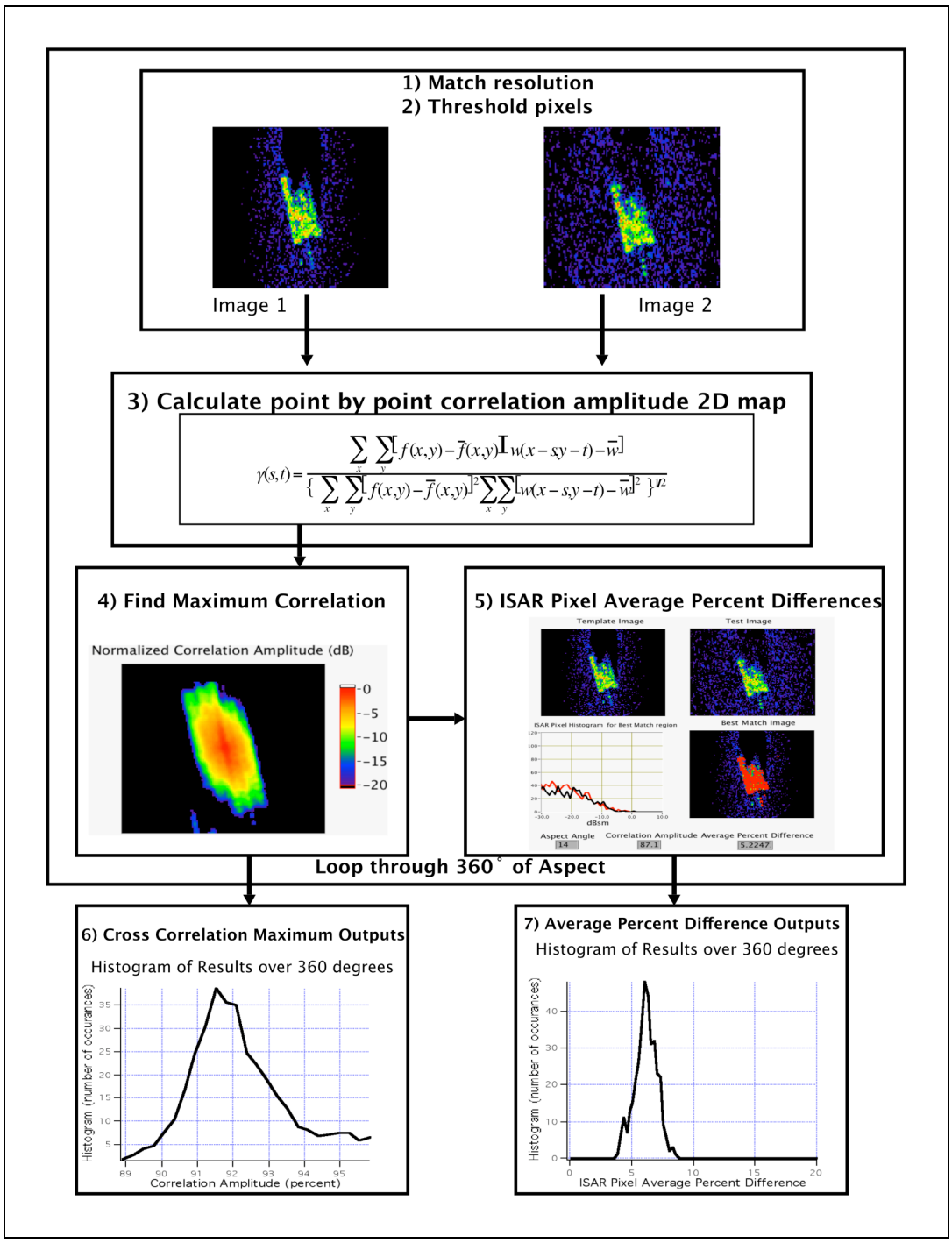

Figure 3.1: Flow chart of the ISAR image analysis.

3.1 Step 1. Match ISAR image resolution

Since the data sets used in this study have been taken on three different radar platforms, using three different scale factors, it was necessary to ensure that the resolution of the ISAR images were identical. The data set with the lowest resolution was able to form 6" pixels, therefore all of the ISAR images used in this study consist of 6" down-range x 6" cross-range pixels. The analysis is programmed to automatically adapt to different data sets and form, as best as possible, the desired 6"x6" resolution. The images are formed by applying a Discrete Fourier Transform (DFT) on both the frequency and azimuth axis. Although it was not always possible to achieve an exact match in resolution between the data sets, it was found that any differences that did occur were negligible. No further numerical techniques such as interpolation of the data were found to be necessary.

3.2 Step 2. ISAR image pixel threshold

After formation of the ISAR images a lower threshold limit must be selected to facilitate the cross correlation analysis. Since several of the data sets in this study consist of targets on ground terrain, a lower limit ISAR pixel threshold of –30dBsm was selected for all of the data in this study. At this threshold the scattering from the ground terrain falls below the threshold limit and is therefore excluded from the analysis. ISAR image pixels are represented in units of dBsm. Data points that fall below the noise threshold are set to the threshold. The absolute value of the threshold is then added to the ISAR pixels. The image that is produced therefore consists of a dB scale where pixels that were originally at or below the threshold limit are now equal to 0 and will have zero weight in the cross correlation analysis described in Section 3.3.

3.3 Step 3. Calculate cross-correlation 2D map.

The two ISAR images to be correlated are represented by the functions *f(x,y)* and *w(x,y)*. The sizes of the 2-D arrays are MxN and JxK respectively. The correlation function between the images is,

$$c(s,t) = \sum_x \sum_y f(x,y) w(x-s, y-t) \tag{1}$$

where s=0,1,2,…M-1 and t=0,1,2,…N-1. The sum in Equation(1) is taken over the overlap region between *f(x,y)* and *w(x,y)*. In order to eliminate sensitivity to changes in the amplitudes of *f(x,y)* and *w(x,y)* it is useful to use a normalized version of Equation(1) as is shown in Ref [4]. This normalization yields the correlation coefficient given in Equation(2).

$$\gamma(s,t) = \frac{\sum_x \sum_y \left[f(x,y) - \overline{f}(x,y) \right] \left[w(x-s, y-t) - \overline{w} \right]}{\left\{ \sum_x \sum_y \left[f(x,y) - \overline{f}(x,y) \right]^2 \sum_x \sum_y \left[w(x-s, y-t) - \overline{w} \right]^2 \right\}^{1/2}} \tag{2}$$

where s=0,1,2,…M-1 and t=0,1,2,…N-1, $\overline{w}$ is the average value of pixels in *w(x,y)* (computed only once), and $\overline{f}(x,y)$ is the average value of *f(x,y)* in the current overlap region. It is useful to note that the correlation coefficient function is scaled in the range –1 to 1.

While the correlation of the ISAR images using Equation (2) is straightforward, it is also numerically intensive to perform a point-by-point numerical integration especially on large ISAR scenes. For this reason it is much more efficient to perform the mathematical correlation by switching to Fourier space. It is well known that a cross-correlation consisting of an integration in image space is equivalent to a simple multiplication in Fourier Transformed space. The images were therefore Fourier transformed, multiplied together, and then transformed back. This allowed the calculation of the entire 2-D cross-correlation amplitude map, which is seen in step 4 of Figure 3.1. Using this technique the speed at which the correlation amplitudes can be calculated is increased by two orders of magnitude.

Although we have been able to calculate only a small subset of correlation amplitudes in previous papers, the entire correlation map is now calculated and stored to disk for further examination. A detailed discussion of the 2-D correlation map is presented in the following sections.

3.4 Step 4. Find point of maximum correlation.

Registration of the pair of ISAR images was assumed to occur where the calculated correlation amplitude was at its maximum. The 2-D correlation map was searched and its peak location was found. This location was then used to overlay the two images on top of each other, to define the maximum correlation amplitude in the later plots of the correlation results (Step 6 in Figure 3.1), and to find the correct overlap of the two data sets for comparison of ISAR pixel statistics (Step 5 and 7 in Figure 3.1). While this technique proved very reliable and failed on only 2 of the 2520 ISAR image pairs, a detailed examination of the full 2-D correlation map revealed a variety of interesting features that should be able to identify the target much more reliably in complex images. This will be discussed further in Section 4.

3.5 Step 5. Calculate ISAR pixel Average Percent Differences (APD).

The analysis of ISAR images by comparison of the differences pixel-by-pixel has been described in detail in previous works.[1] Therefore, only a brief description will be given here. The ISAR images that result from the threshold method described in Step 2 are overlapped with each other using the location of the maximum correlation amplitude calculated in Step 4. Using an algorithm developed in Ref.(1) the images are compared pixel-by-pixel and a percent difference map is generated where the absolute value of the differences is taken to provide a measure of deviation between the two images. The average of the absolute percent differences are taken across the entire image to yield a single Average Percent Difference (APD) value for each ISAR image pair.

3.6 Step 6. Maximum cross-correlation outputs over 360 degrees.

Steps 1 through 5 are repeated at 1˚ increments in azimuth angle for the full 360˚ spin of the target data set. The value of the maximum cross-correlation at each azimuth angle is output into an array of maximum correlation amplitudes. A histogram of this array is formed to show the statistical spread of the maximum correlation amplitudes. Figures 3.2 and 3.3 show typical plots of the maximum correlation amplitude as a function of angle and the corresponding histogram derived from it.

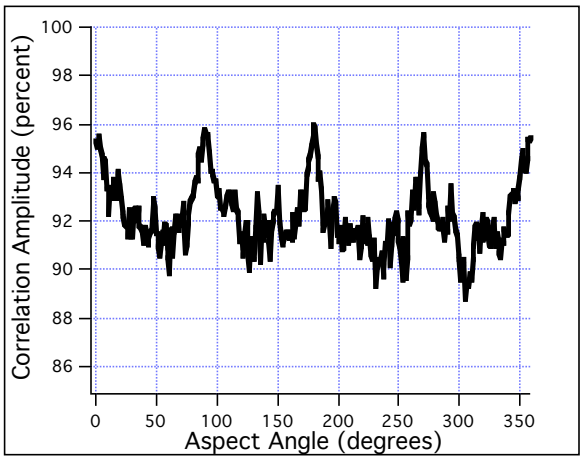

Figure 3.2 Typical VV maximum correlation amplitudes

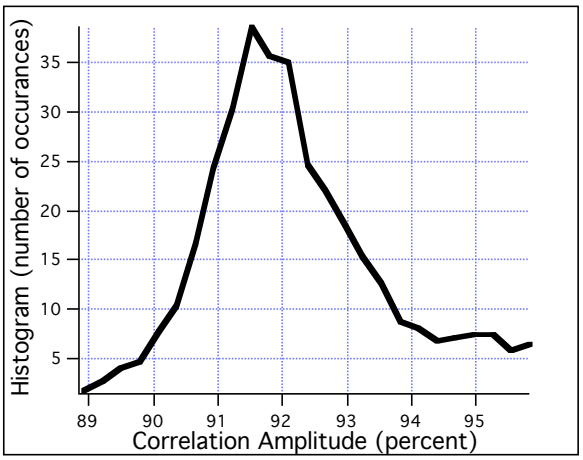

Figure 3.3 Histogram of maximum correlation amplitudes.

3.7 Step 7. ISAR pixel average percent difference outputs over 360 degrees.

A procedure similar to Step 6 is performed on the APD outputs as a function of azimuth angle with the resulting histograms of the APDs being output.

4. RESULTS

4.1. Cross-correlation and Average Percent Difference results.

The outputs generated using the methods described in Sections 3.1-3.7 are shown in Figures 4.1 and 4.2 for the cross-correlation coefficient and ISAR pixel average percent differences respectively. In this study a single data set was chosen to be correlated against all other data sets. The histograms of Figures 4.1 and 4.2 show the correlation of the 1/35th scale T72 data set taken on a desert terrain ground plane (Table 1, data file 1) against all other data sets. The data are separated into two classes in the upper and lower graphs of the figures for easier display. The upper graphs for both figures display the results of correlating the T72 data set with other T72 data sets regardless of exact configuration, multi-target scene, and scale factor. The lower graphs of both figures show the results of correlating the T72 with other targets of similar size (Table 1, data files 7 and 8).

It is useful to first consider the cross correlation histograms of Figure 4.1(upper). The light blue curve shown in the upper graph of Figure 4.1 shows the test case of the 1/35th scale T72 correlated against itself using two separate data runs. The files were collected by measuring the T72 through 720˚of azimuth. The first 360˚ were then correlated with the second 360˚. It is not surprising that the results show a nearly perfect match with a correlation amplitude of nearly 100% and an ISAR image APD of almost 0% difference, as seen in Figure 4.2(upper).

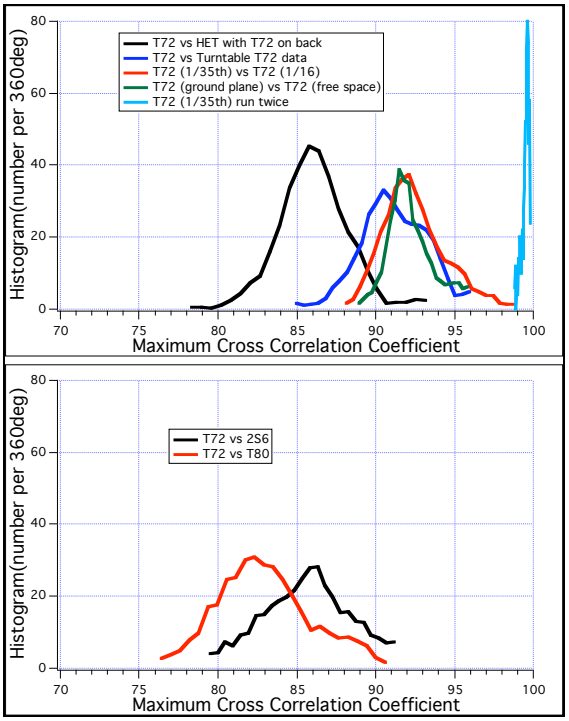

Figure 4.1. Histograms of correlation values. Upper graph show T72 verses other T72 data sets. Lower graph shows T72 verses other targets.

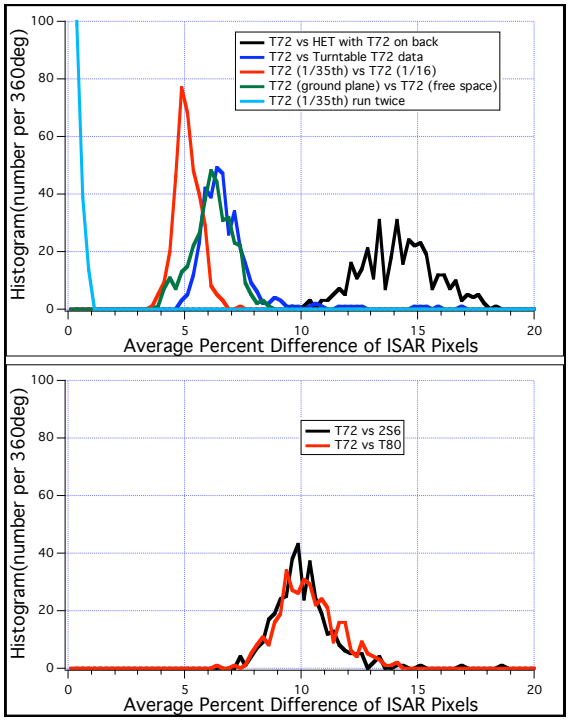

Figure 4.2. . Histograms of pixel difference values. Upper graph show T72 verses other T72 data sets. Lower graph shows T72 verses other targets.

Examining the next best correlation amplitude matches in Figure 4.1(upper) it can be seen that the matching of the T72 data set to the 1/16th scale T72, full-scale T72 and 1/35th scale T72 in free-space show virtually identical matches of about 93% in correlation amplitude. Examining Figure 4.2(upper) it is noted that the differences in ISAR pixel amplitudes are the smallest (less than 5%) between the 1/35th scale and 1/16th scale data sets. This result is due to the fact that the 1/35th scale model was constructed with an attempt to copy as much of the detail of the 1/16th scale model as could easily be done but not to provide an exact duplicate and therefore has some small configuration differences. Slightly larger pixel differences were observed when matching the T72 on a ground plane to the same target in free

space and matching it to the full-scale data set. The average differences were both on the order of 6%. This result is consistent with results seen in previous works (Ref.(2)) that demonstrate the RCS variability of targets in operational environments. It is useful to remember that the 1/35th scale T72 has some configuration differences compared to the full-scale T72 and additionally they were taken in the far field and near field respectively. These differences are sufficient to account for the change in APD. Even with the difference in configuration between the data files it is clear that the T72 data sets taken across 3 different platforms (1/35th, 1/16th, and Full-scale) correlate very well with large correlation amplitudes and small APD values being measured. The comparison of the T72 on the ground plane with the same target on the back of the Heavy Equipment Transporter (HET) showed both the smallest correlation amplitude (86%) in Figure 4.1(upper) and the largest change in pixel RCS (14%) as seen in Figure 4.2(upper). This is due to the significant change in scene by placing it on top of another target. The results of the HET correlation will be discussed further in the next section.

Examining the curves in the lower graphs of Figures 4.1 and 4.2 show how the T72 compares against the 2S6 air defense unit and the T80 MBT. It is not surprising that the correlation amplitudes of these targets are the lowest (82%) and that the pixel APD is now 10%. This result is also consistent with previous works (Ref.(2)) for correlation against the wrong target. It is somewhat surprising that the comparison of the T72 with the same target on the HET shows a comparable APD to that obtained from comparing different targets. This result seems to indicate that for a complex two-target scene the true target will be very difficult to match if only the maximum amplitude of the cross-correlation is considered. However, an examination across the entire scene of the 2-D correlation map that is generated in Step 3 of Figure 3.1 shows several interesting features that may aid significantly in target identification. The results are discussed in the next section.

4.2. 2-D correlation maps of the T72 verses the HET.

After reviewing the results of Section 4.1 an attempt was made to determine the cause of the large change in correlation amplitude and APD of the T72 data set compared to the T72 mounted on the HET. It was observed that the change can be accounted for by two dominant affects. The most significant one is the increase in scattering on the T72 due to interactions with the HET that had a tendency to raise the ISAR pixel RCS locally. The next affect was caused by shadowing of the T72 by the various parts of the HET with the largest shadowing being observed by the truck cab. Figures 4.3 and 4.4 show typical examples of the comparison of the T72 alone to the T72 on the HET. In these figures the best match region is marked in red, and a comparison of the images shows both the effect of shadowing and the target interaction.

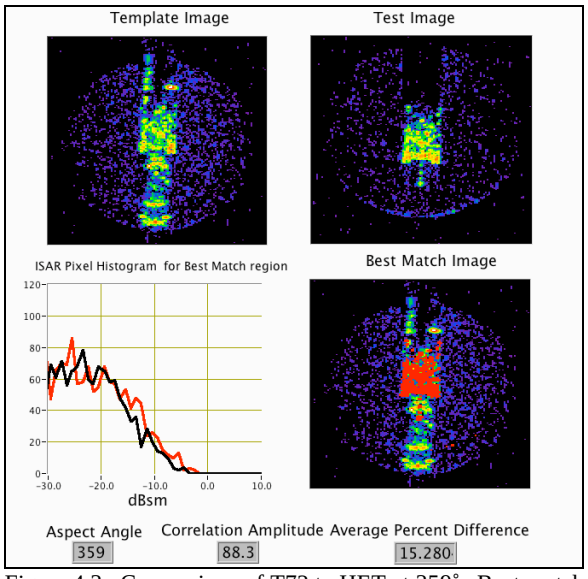

Figure 4.3. Comparison of T72 to HET at 359˚. Best match region is marked in red.

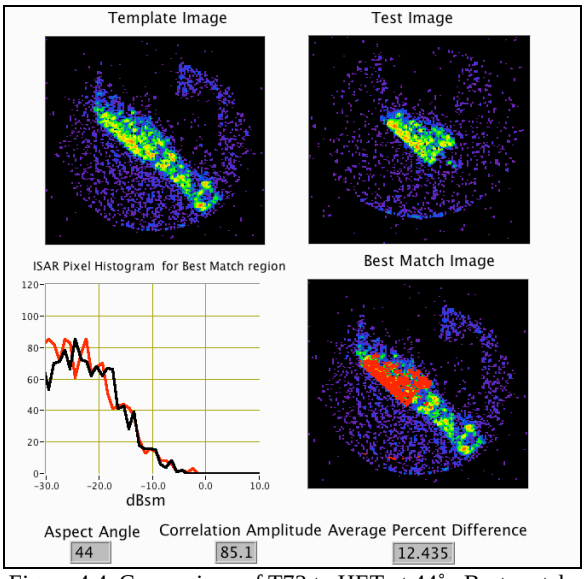

Figure 4.4. Comparison of T72 to HET at 44˚. Best match region is marked in red.

Calculation of the 2-D cross correlation map (MAP) has been described in Section 3.3. A single MAP is generated when 2 individual ISAR images are correlated, such as the correlation of the test and template images shown in Figure 4.3. This MAP is a 2-D array with the 3rd dimension being the value of the correlation and can be plotted using a 3-D display. Figure 4.5 shows the 3-D plot of several MAP surfaces at various angles with x and y on the bottom axes (the down-range and cross-range coordinates) and z being the value of the correlation amplitude in dB. A preliminary look at Figure 4.5 shows that there are several local maxima distributed through the MAP that represent the fact that it is a correlation across a large complex scene. In Figures 4.5 (a, b, and d) the maximum peak occurs on a very sharp feature in the MAP where the T72 test image overlaps the position on the back of the HET that corresponds to where the T72 is mounted. In Figure 4.5c the larger peak amplitude occurs at the cab of the HET and not the T72 where the technique of picking the largest correlation amplitude failed to identify the correct spot. This is the very broad peak at the right of Figure 4.5c. However, there still exists a very sharp peak where the real T72 is located, although its absolute amplitude is lower. It has been found that in this large complex scene a very sharp peak always occurred where the real target was located, regardless of its relative amplitude. This sharp peak does not appear to broaden significantly even when the peak amplitude and APD changed by very significant amounts. In the next section a similar comparison will be made between the data sets for all of the targets.

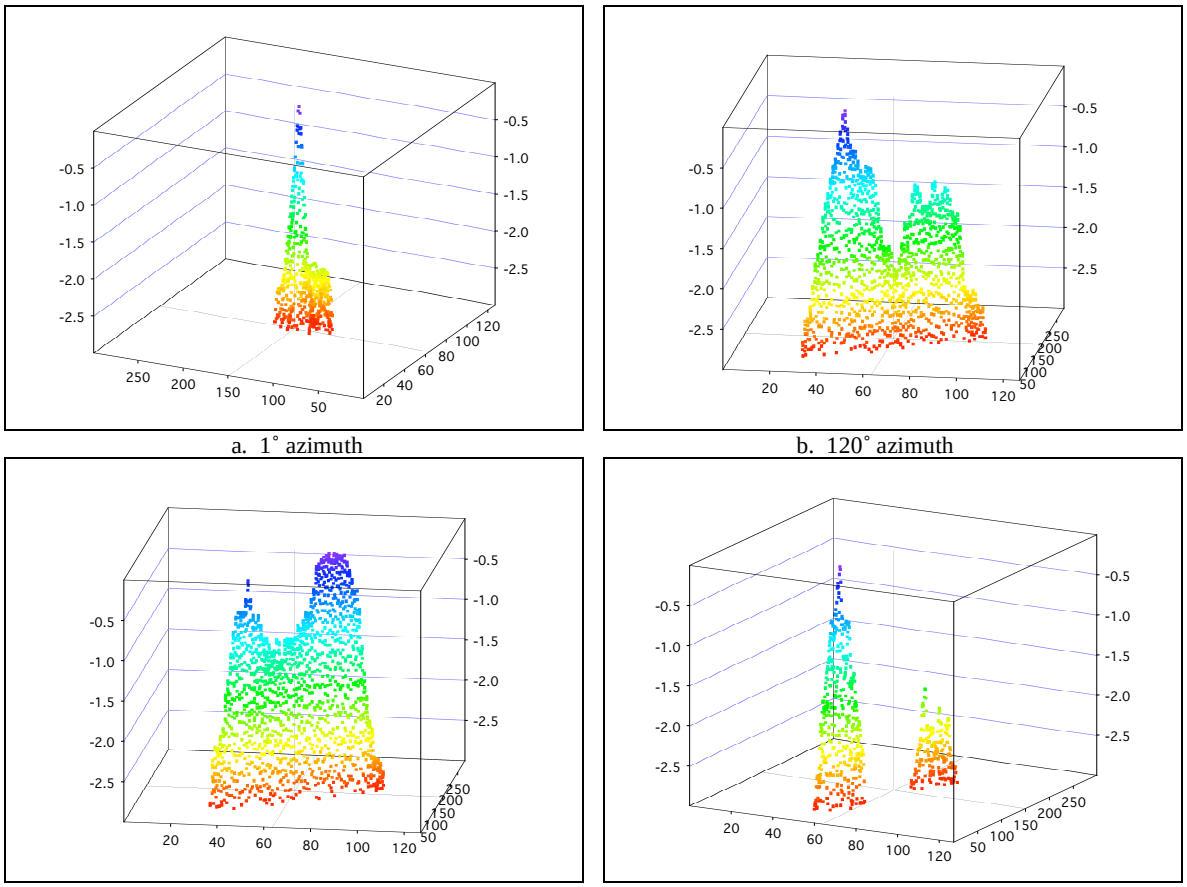

a. 1˚ azimuth b. 120˚ azimuth

c. 126˚ azimuth d. 160˚ azimuth

Figure 4.5. Two-dimensional correlation maps of the T72 verses the Heavy Equipment Transporter with the T72 mounted on the back (dB scale).

4.3. Comparison of all 2-D cross-correlation maps.

Since sharp peaks in the MAP data sets were seen to be a persistent feature for the correlation against the HET data sets, a limited study of the MAP data for all other targets was performed to determine if similar features could also be seen. Figure 4.6 shows at individual angles the 3-D plots of the MAP calculation for the 1/35th scale T72 verses the 1/35th,

1/16th, full-scale T72, T72 on HET, 2S6 and T80. It is easily seen that the MAP of the 1/35th scale verses 1/35th-scale T72 data sets shows the sharpest peak. The next sharpest peak is seen in the MAP of the 1/16th scale data set which is perhaps not surprising since they also showed the smallest differences in correlation amplitude and APD. It is difficult to quantify the level of sharpness for the HET MAP since it contains the peaks from multiple parts of the complex two-target scene but it appears that its peaks and that of the full-scale data set have about the same sharpness. The MAP of the 2S6 and the MAP of the T80, however, show a different shape for the peaks that appear to broaden out when compared to the correlation of the T72 data sets.

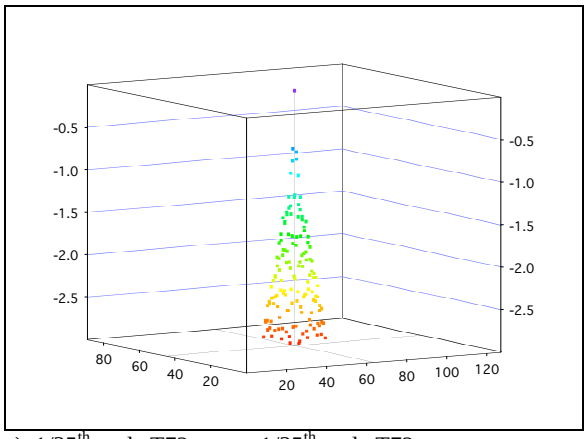

a) 1/35th scale T72 verses 1/35th scale T72

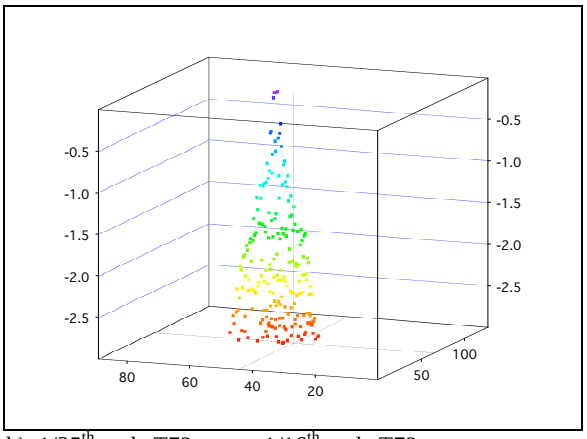

b) 1/35th scale T72 verses 1/16th scale T72

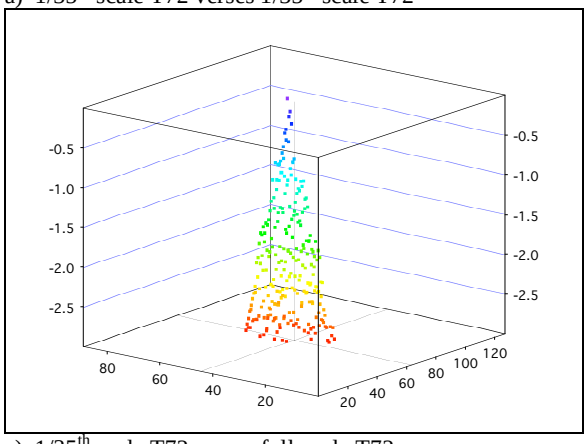

c) 1/35th scale T72 verses full-scale T72

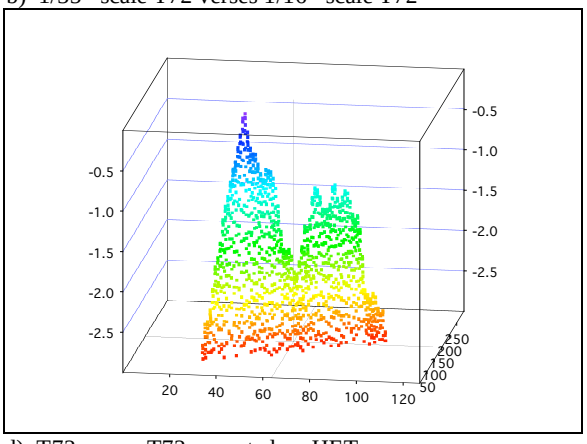

d) T72 verses T72 mounted on HET

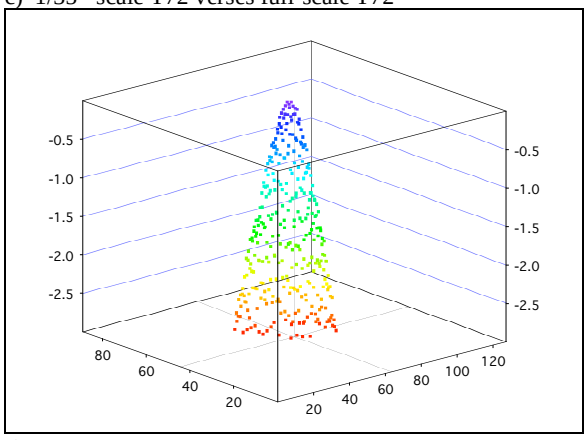

e) T72 verses 2S6

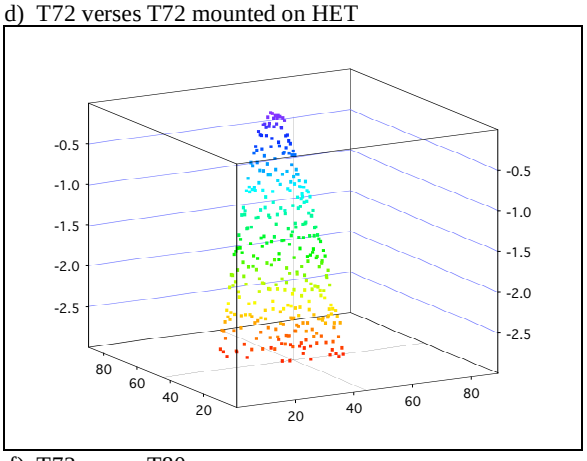

f) T72 verses T80

Figure 4.6. Two-dimensional correlation maps of the T72 verses all targets (dB scale).

Since the data shown in Figure 4.6 are plotted in dB, the images tend to make real differences appear to be more compressed on the z-axis. Figure 4.7 shows the same MAPS for the 1/35th scale T72 verses Full-scale (Fig. 4.7a) and the T72 verses 2S6 (Fig. 4.7b) plotted now in linear scale. From Figure 4.7 it appears that there is a change in shape that occurs that is dependant on whether the match is against the same target or against the wrong target. The results in Figure 4.6 suggest that this may be a trait that is common across radar platforms and target scene configurations, although more research into the exact nature of this effect needs to be done.

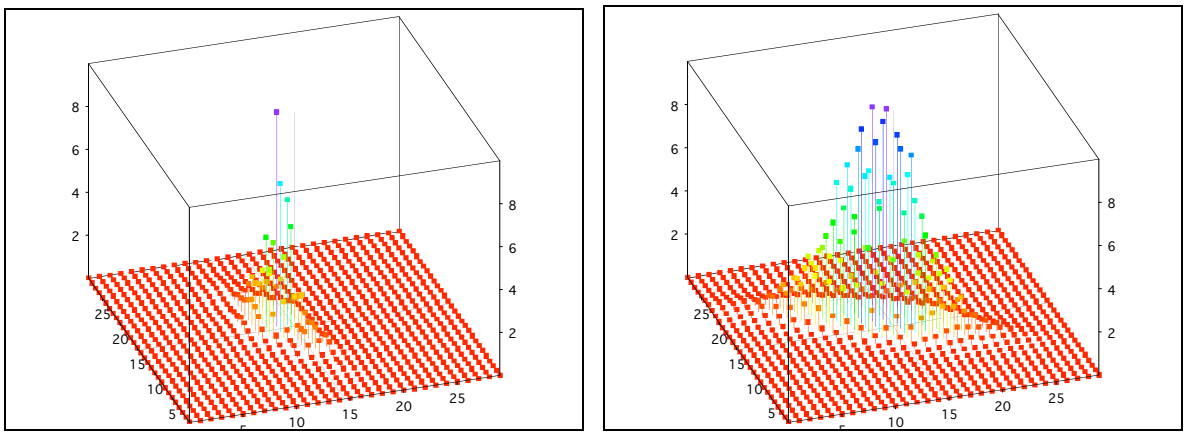

Figure 4.7 Two-dimensional correlation maps of the 1/35th scale T72 verses Full-scale T72 (a), and 1/35th scale T72 verses 2S6(b) (linear scale).

5. SUMMARY

High resolution ISAR imagery has been analyzed using a cross-correlation technique and the ISAR pixels have been compared between images by calculating the pixel-by-pixel average percent differences. It has been shown that the cross-correlation of ISAR data sets on a T72 target give very good matches across 3 separate platforms (full-scale, 1/16th-scale, and 1/35th-scale), with variations in the matches attributable to differences in target configurations and radar illumination. Furthermore, a complex two-target scene was studied with the 1/35th-scale T72 tank model mounted on the back of a heavy equipment transporter. Upon close examination of the 2-D cross-correlation map it has been observed that there are sharp features in the shape of the correlation map at the locations where the real target is matched. These features have been observed across all three platforms and various target configurations. It is therefore proposed that a detailed shape analysis of the correlation maps may provide a more reliable way to identify the target, even when imbedded in a complex scene.

REFERENCES

1. R.H. Giles, W.T. Kersey, M.S. McFarlin, B.G. Woodruff, R. Finley, W.E. Nixon,"*Multiple-resolution study of Ka-band HRR polarimetric signature data*", Proc. SPIE Vol. 4050, p. 408-417, Automatic Target Recognition X; Firooz A. Sadjadi; Ed. August 2000
2. R.H. Giles, W.T. Kersey, A.J. Gatesman, M.J. Coulombe, S. McFarlin, W.E. Nixon, R. Finley,"*X-band radar signature characteristics for main battle tanks in operational environments*", Proc. SPIE Vol. 4718, p. 336-343, Targets and Backgrounds VIII: Characterization and Representation; Wendell R. Watkins, Dieter Clement, William R. Reynolds; Eds. August 2002
3. R.H. Giles, W.T. Kersey, M.S. McFarlin, H.J. Neilson, R. Finley, W.E. Nixon,"*Target variability and exact signature reproduction requirements for Ka-band radar data*", Proc. SPIE Vol. 4380, p. 117-126, Signal Processing, Sensor Fusion, and Target Recognition X; Ivan Kadar; Ed. August 2001
4. R. C. Gonzalez and R. E. Woods, *Digital Image Processing*, p583-584, Addison-Wesley Publishing, Reading Massachusetts, 1992.